JOURNAL OF MATERIALS SCIENCE **34** (1999) 2389–2400

Comparison between crystal field effects on the fluorescence spectra of crystalline SmP_5O_{14} and vitreous $(Sm_2O_3)_{0.248}(P_2O_5)_{0.752}$

H. M. FAROK, G. A. SAUNDERS
School of Physics, University of Bath, Claverton Down, Bath, BA2 7AY, UK

W. C. K. POON, J. CRAIN, H. VASS
Department of Physics, The University of Edinburgh, James Clark Maxwell Buildings, Mayfield Road, Edinburgh, EH9 3JZ, UK

W. HÖNLE, E. SCHÖNHERR
Max-Planck-Institut für Festkörperforschung, Heisenbergstrasse 1, 70569 Stuttgart, Germany

To investigate how the local symmetry of the Sm^{3+} ion affects the fluorescence of a samarium metaphosphate glass of composition $(Sm_2O_3)_{0.248}(P_2O_5)_{0.752}$, the temperature and pressure dependences of its laser induced fluorescence spectrum are compared with those of a samarium pentaphosphate crystal (SmP_5O_{14}). Findings include: (i) The crystal field splitting of the energy levels responsible for fluorescence in SmP_5O_{14} at room temperature is consistent with the local symmetry of oxygen atoms of the phosphate cage around the Sm^{3+} ions being quite close to cubic – in accord with crystal structure. At 12 K there is a systematic disappearance of the shortest wavelength lines of each fluorescence band attributable to a decreasing population of higher crystal field levels, which are occupied at ambient temperature. (ii) The $(Sm_2O_3)_{0.248}(P_2O_5)_{0.752}$ glass fluorescence spectrum forms five bands, which can be related to that of the crystal but with inhomogeneous line broadening; the short wavelength edges sharpen at low temperatures, also attributable to a decreasing population of higher crystal field levels at lower temperatures. (iii) The shifts ($d\lambda/dp$) in the wavelengths of the fluorescence peaks of the SmP_5O_{14} crystal induced by pressure up to 50 kbar in a diamond anvil cell are small but measurable at room temperature, being about $+0.03\,nm\,kbar^{-1}$ ($+0.3\,Å\,kbar^{-1}$). Application of pressures up to 50 kbar to the $(Sm_2O_3)_{0.248}(P_2O_5)_{0.752}$ glass did not alter the positions of the bands within the error in the fluorescence wavelength measurements. Neither the SmP_5O_{14} crystal nor the metaphosphate glass showed any indication of undergoing a phase transition up to the highest pressure reached. A low frequency Raman mode has been observed, which softens with reducing temperature, indicating softening of the associated optical mode and suggesting that, like other RP_5O_{14} crystals, SmP_5O_{14} undergoes a ferroelastic phase transition.

1. Introduction

Rare earth metaphosphate glasses having compositions in the vicinity of $(R_2O_3)_{0.25}(P_2O_5)_{0.75}$ (where R represents one of the rare earth elements) become strongly magnetic at low temperatures [1–3]. Below about 10 K the specific heats of the metaphosphate glasses containing Sm^{3+} and Gd^{3+} ions increase considerably, becoming three orders-of-magnitude larger in the Gd^{3+} glass than in the diamagnetic La^{3+} glass [1], a magnetic contribution larger than any found previously for an oxide glass. Novel magnetic and magneto-optic phenomena occur in these glasses, which contain very large concentrations of magnetic ions [1]. In general low-energy excitations having a wide distribution of energies due to the random structural disorder are a universal feature distinguishing amorphous solids from crystalline counterparts. They are the origin of characteristic optical, thermal and acoustic properties of glasses in both the low-temperature regions below and above 1 K [4, 5]. The scope of this fundamental behaviour of the glassy state has even wider applicability, extending to the existence of a wide spectrum of low-lying magnetic excitations, which is responsible for magneto-optical effects such as a wide band in the low-frequency Raman spectrum of Pr^{3+} metaphosphate glass [1]. Magnetic glasses have a plethora of fascinating physical properties of fundamental interest and potential application in laser and optoelectronics technology. In general the rare earth dopant incorporated into a glass matrix provides the electronic energy level structure required for

non-linear optical devices. Learning more about the local structure around rare earth ions, and how it relates to optical absorption and fluorescence, is essential for understanding and using the magnetic and magneto-optical properties of these rare earth metaphosphate glasses.

In general rare earth ions incorporated in glasses tend to show optical absorption and fluorescence spectra having characteristics found for rare earth ions in inorganic crystals but with inhomogeneous line broadening due to a multiplicity of rare earth sites in a glass [6, 7]. Hence to extend understanding of the Sm^{3+} metaphosphate glass fluorescence, it is compared here with fluorescence determined as a function of temperature and pressure for a single crystal of samarium pentaphosphate (SmP_5O_{14}), which like the metaphosphate glass is constructed from linked phosphate groups [8]. The RP_5O_{14} compounds are themselves luminescent crystalline materials with interesting optical properties, which have possible uses in optical communication systems [9, 10].

The 4f electrons, screened by outer shell electrons, are responsible for the characteristic spectra of trivalent rare earth ions; spectral studies can provide direct information about their energy levels in crystals and glasses. Alternatively, an ion can be used as a probe to determine and measure the type and strength of the crystalline field [11]. The association between local structure and fluorescence properties of glasses doped with small concentrations of rare earth ions (but not the metaphosphates, which contain a very high modifying ion content) has previously been used to provide information about laser glasses [12, 13]. A broad-brush picture is that their optical absorption and fluorescence spectra consist of line multiplets in "bands" separated by a wave number difference of the order of $1000\,cm^{-1}$; within such a band the lines result from transitions to a multiplet of levels having the same total angular momentum, J, and are of the order of $100\,cm^{-1}$ apart. In the case of samarium metaphosphate glass previous fluorescence and optical absorption studies have shown that the valence state of samarium is three: the line positions found are those expected from transitions between the $4f^5$ electron energy levels of Sm^{3+} [14].

A rare earth ion incorporated in a glass or crystal matrix is subjected to the crystal field of the surrounding ions, so that the Stark effect splits each single level of the free ion into a group of levels. Using group-theoretical methods, Bethe [15] determined the number of levels produced by crystal field splitting from a given free ion level. Runciman [16] classified the 32 crystallographic point groups under four categories: cubic, hexagonal (including the hexagonal and rhombohedral systems), tetragonal, lower symmetry (including orthorhombic, monoclinic and triclinic). Laser induced fluorescence studies have been used here to relate the local symmetry of the Sm^{3+} ion in the crystalline and glass matrices to the Runciman classification. Due to topological disorder the environment of a fluorescent ion is not sufficiently well defined to enable a simple characterization of optical properties of an amorphous solid: the observed emission consists of a superposition of contributions from individual ions distributed among the entire ensemble of local environments. The resulting statistical distribution of Stark components brings about substantial inhomogeneous line broadening, limiting attempts at interpretation. By contrast, sharp lines characterize the crystal fluorescence; these have been used here in an examination of crystal field effects due to the local structure surrounding the Sm^{3+} ions in the SmP_5O_{14} crystal and the criteria developed carried over to explore the local environment of the Sm^{3+} ions in a metaphosphate glass of composition $(Sm_2O_3)_{0.248}(P_2O_5)_{0.752}$. The study includes examination of the effects of high pressure and low temperature on the fluorescence spectra of the glass of composition $(Sm_2O_3)_{0.248}(P_2O_5)_{0.752}$ and crystalline SmP_5O_{14}.

2. Experimental procedure

The samarium metaphosphate glasses were made from laboratory reagent 99.9% purity grades of phosphorus pentoxide (P_2O_5) and samarium oxide (Sm_2O_3) [17]. The mixed oxides were reacted in quantities of about 50 g by heating for about 1 h at 500 °C in a closed alumina crucible in an electric furnace. The mixture was then melted in a second furnace and held for 1 h at 1400 °C. After stirring, the melt was cast into a preheated (500 °C) split, steel mould to make a glass cylinder 10 mm long and 14 mm in diameter. Following casting, the glass was immediately transferred to an annealing furnace at 500 °C and kept there for 24 h, after which the furnace was switched off and the glasses were left to cool down to room temperature, at a cooling rate of $0.5\,°C\,min^{-1}$. The glasses were transparent, yellow in colour and of optical quality. Samples were polished to have flat and parallel faces to within 10^{-3} radian for the optical measurements.

The compositions of the glass samples were determined by quantitative analysis using a Jeol JXA-8600M electron probe microanalyser (EPMA) fitted with wavelength dispersive spectrometers (WDS). A pure crystal of SmS was used as a standard. The microanalyser was fitted with four double-crystal spectrometers, which could be used to analyse the X-ray spectrum of the elements present in the glass. Using this technique, the electron beam could be directed at a relatively small area without destroying the sample. Fourier transform infrared (FTIR) analysis of the glass showed no indication of OH^- groups within experimental sensitivity: they can be present only in a concentration of less than 0.1 mol % (corresponding to a number of about $10^{19}\,cm^{-3}$).

Crystals of SmP_5O_{14} were grown from a H_3PO_4–Sm_2O_3 solution in a vitreous graphite crucible. Sm_2O_3 powder was added to about 200 g 85% H_3PO_4 acid in a weight proportion of 7.81×10^{-3}. The crucible was covered with a vitreous graphite plate. The mixture was slowly heated to 500 °C at a constant rate of $8.3\,°C\,h^{-1}$ in air. At 500 °C rhombically shaped crystals of SmP_5O_{14} appeared within 700 h on the crucible walls. When small crystals of about 1 mm in length were used as seed, large crystals up to 7 mm in length and 2 mm in thickness could be obtained. The seed crystals were inserted in the hot solution after it had reached 500 °C. The crystals were isolated by decanting the hot acid.

The low temperature fluorescence spectra of the crystal and glass were excited using the 476.5 nm (4765 Å) blue line of an argon ion laser. The specimens were contained in a cryostat capable of reaching 10 K with temperature control to ±1 K. The exciting laser power was varied from 50 to 200 mW depending on the resultant fluorescence intensity in the specified spectral region. The fluorescence scattered at 90° to the laser beam was collected and focused into a triple grating monochromator with input and exit slit widths set to 100 μm for the SmP_5O_{14} crystal and at 150 μm for the glass.

The Raman spectrum of the samarium pentaphosphate (SmP_5O_{14}) crystal was measured and recorded at 12 and 300 K. The spectrum was obtained using the 488 nm (4880 Å) argon ion laser line with 200 mW lasing power, 200 μm slit widths, and scanning steps of 1 cm^{-1} for every 3 s. The frequency shifts of the Raman lines were measured to an accuracy of ±1 cm^{-1}.

To make fluorescence spectra measurements of the SmP_5O_{14} crystal and $(Sm_2O_3)_{0.248}(P_2O_5)_{0.752}$ glass under high pressure at room temperature, a different optical system was used. A single grating monochromator (Rank-Hilger 1200 lines mm^{-1}) was employed with its slit widths set at 200 μm in the case of the glass and 100 μm in the case of the crystal. The fluorescence spectra of the SmP_5O_{14} crystal and $(Sm_2O_3)_{0.248}(P_2O_5)_{0.752}$ glass were obtained by exciting with the same argon ion laser line, 476.5 nm (4765 Å). For the crystal, the laser power varied from 100 mW under atmospheric pressure to 250 mW for 50 kbar pressure. For the glass the laser power varied from 150 mW for the atmospheric pressure, to 300 mW for the 50 kbar pressure. The pressure was generated by a standard diamond anvil cell (DAC). The gasket in the DAC was made of hard stainless steel, 0.3 mm thick, with a 0.35 mm diameter hole drilled in its centre. A sample of about 100 μm was placed in the gasket hole. It was accompanied by a chip of ruby of about 50 μm in size for pressure measurement [18, 19]; a 4 : 1 methanol–ethanol liquid mixture comprised the hydrostatic pressure medium. The pressure level in the DAC was determined by measuring the shift of the ruby 694.2 nm (6942 Å) fluorescence line and using the calibration equation $d\lambda/dp = 0.0365$ nm $kbar^{-1}$ (0.365 Å $kbar^{-1}$) [19]. The fluorescence spectra were recorded at various pressures up to 50 kbar in steps of about 5 kbar. To ensure high resolution and accurate measurement of the ruby calibration line, the optical slit widths were set at 50 μm, which enabled accurate determination of the pressure exerted in the DAC. The error in the pressure measurement was ±1 kbar and the experimental error in wavelength measurement was ±0.2 nm (±2 Å).

3. Results and discussion

3.1. Comparative study of the fluorescences of SmP_5O_{14} and $(Sm_2O_3)_{0.248}(P_2O_5)_{0.752}$ glass

3.1.1. Fluorescence spectrum of crystalline SmP_5O_{14}

The crystalline rare earth pentaphosphates can have three types of structure [8]. The crystal structure of SmP_5O_{14}, determined at ambient conditions on single crystals by X-ray crystallography, is monoclinic; there are four SmP_5O_{14} formula units in the unit cell [space group $P2_1/c$, all atoms being located on 4(e) Wycoff sites] with $c = 1.299$ nm (12.990(6) Å), $b = 0.894$ nm (8.944(4) Å), $a = 0.875$ nm (8.750(4) Å) and $\beta = 90.45(10)^\circ$ and density 3450 kg m^{-3} at ambient temperature. Along the a-axis the $(P_5O_{14})^{3-}$ anions form infinite one-dimensional double chains consisting of two different eight-membered rings of linked PO_4 tetrahedra. These chains are bound together by the Sm^{3+} cations, which are co-ordinated in the form of quadratic antiprisms with 0.2354 nm (2.354 Å) ≤ d(Sm–O) ≤ 0.2487 nm (2.487 Å). There is strong deformation of the individual PO_4 tetrahedra. The crystal structure is illustrated in Fig. 1. Of particular interest for the present discussion is the local environment of the Sm^{3+} ion; the nearest neighbours of the Sm^{3+} ion are shown in side view (a) and in top view (b). The first co-ordination shell of the Sm^{3+} ion is comprised of eight oxygen atoms at a distance of between 0.235 and 0.249 nm (2.35 and 2.49 Å). Each of the near-neighbour oxygen atoms is associated with a distinct PO_4 unit, some of which are also shown in Fig. 1. Under ambient conditions the co-ordination polyhedron of the Sm^{3+} ion is an approximately square (archemedian) anti-prism (Fig. 1c) with the rare earth species in the centre and the eight oxygen atoms on the vertices. The nearly square faces have side lengths ranging from about 0.282 to 0.3 nm (2.82 to 3.0 Å). The angles associated with these faces range from 85.5 to 93.7°.

Both crystalline SmP_5O_{14} and the $(Sm_2O_3)_{0.248}$ $(P_2O_5)_{0.752}$ glass are strongly fluorescent, the crystal rather more so than the glass. The fluorescence spectra of the SmP_5O_{14} crystal measured at 12 and 300 K at atmospheric pressure are shown in Fig. 2. The electronic configuration of the Sm^{3+} ion is $4f^5$ and the visible fluorescence spectrum originates mainly from the transitions between the $^4G_{5/2}$ level to the ground ^6H multiplet. Electrons in 4f shells in the rare earth ions are screened by the outer shell 5d electrons. Thus, the discrete levels for rare earth ions incorporated in crystals or glasses have energies close to those of free ions. The positions of the fluorescence peaks of the SmP_5O_{14} crystal at 12 and 300 K at atmospheric pressure are listed in Table I. When the crystal was cooled down to 12 K, there was no measurable shift in the fluorescence lines. A feature of all the five bands is the disappearance of some of their shorter wavelength lines at low temperature.

The fluorescence spectrum due to the samarium ions in the crystal splits into five groups of well separated bands at around 560, 600, 650, 700 and 770 nm (5600, 6000, 6500, 7000 and 7700 Å; (Fig. 2). This spectral structure is consistent with a 3+ valence state for the samarium ions: the bands can be attributed to transitions from the $^4G_{5/2}$ level to the lower levels of ^6H_J where J = 5/2, 7/2, 9/2, 11/2 and 13/2 (Table I). The fine structure revealed in these bands is due to crystal field interaction on the free-ion energy levels of Sm^{3+}.

Inspection of the fluorescence spectrum (Fig. 2) and the assignments given in Table I, together with the systematic absences of lines at low temperature (12 K) is

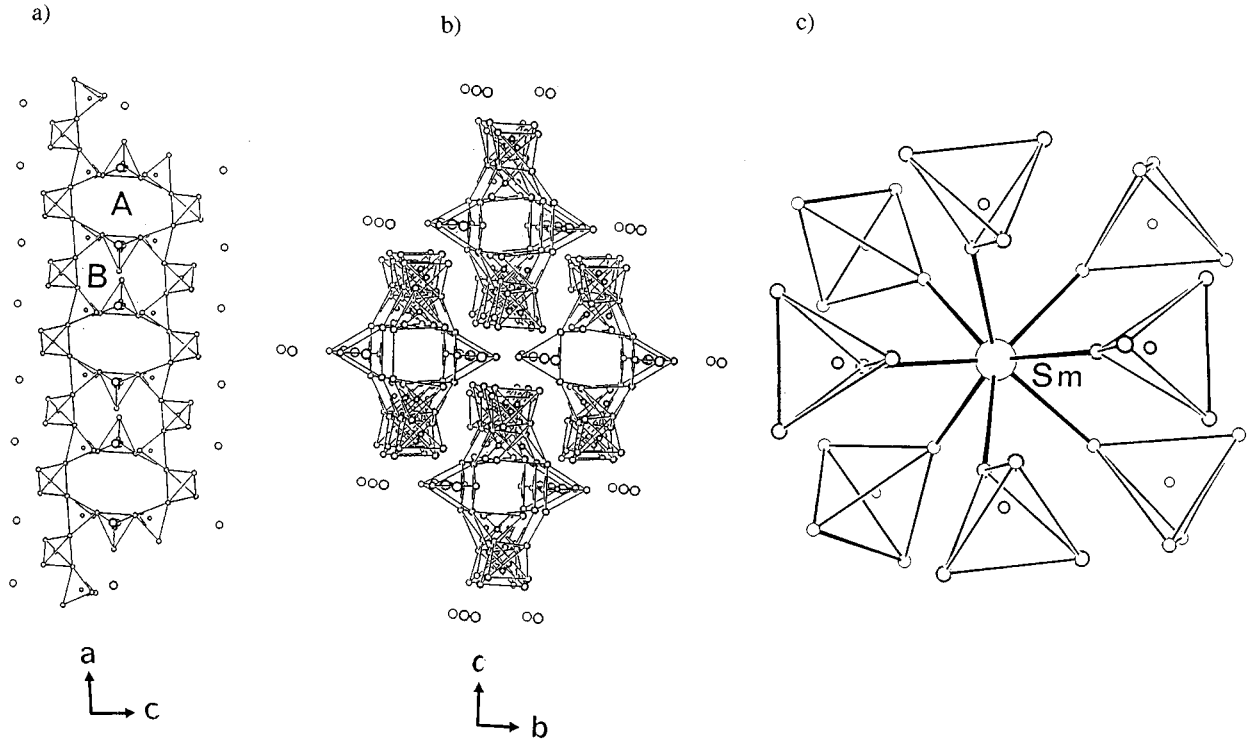

Figure 1 Stereoviews of the crystal structure of SmP_5O_{14}: (a) linked chains of PO_4 tetrahedra–note the different eight-membered rings (labelled A and B) with PO_4 tetrahedra as ring members; (b) arrangement of such chains nearly perpendicular to the (1 0 0) plane; and (c) the co-ordination around a Sm^{3+} ion with the adjacent PO_4 tetrahedra–the bonds between the P atoms are not drawn, instead only the topological lines between the O atoms are shown.

consistent with the local environment of the Sm^{3+} ions (Fig. 1). At room temperature the transition from the $^4G_{5/2}$ level to $^6H_{5/2}$ shows four peaks (dotted line). Four peaks can also be seen in the low temperature (12 K) spectrum (solid line). The transition from the $^4G_{5/2}$ level to the $^6H_{7/2}$ level shows seven peaks at room temperature, but only six peaks at 12 K. The third transition to the $^6H_{9/2}$ level shows about nine peaks at room temperature and six peaks at 12 K. The fourth transition to the $^6H_{11/2}$ level shows what seem to be eight peaks at room temperature and ten peaks at 12 K. The fifth set of transitions to the $^6H_{13/2}$ level indicates that there are probably seven peaks at room temperature and that number also at 12 K. Taking into consideration the term-splitting for the half-integral J of the trivalent samarium ion terms in the Runciman classification [16], there are two options for the local symmetry. The first one is cubic and the second one comprises all the other groups (hexagonal, tetragonal and low symmetry). For the option of the cubic symmetry, the splitting of the terms of the Sm^{3+} ion would be $^4G_{5/2} = 2$, $^6H_{5/2} = 2$, $^6H_{7/2} = 3$, $^6H_{9/2} = 3$, $^6H_{11/2} = 4$, $^6H_{13/2} = 5$, so the expected fluorescence line number would be four in the first band, six in the second band, six in the third band, eight in the fourth band, and ten in the fifth band. For the second option, namely the remaining symmetries, the splitting would be $^4G_{5/2} = 3$, $^6H_{5/2} = 3$, $^6H_{7/2} = 4$, $^6H_{9/2} = 5$, $^6H_{11/2} = 6$, $^6H_{13/2} = 7$, and the expected fluorescence line number in each band would be nine in the first band, 12 in the second band, 15 in the third band, 18 in the fourth band and 21 in the fifth band. A count of the number of lines in each band of the fluorescence obtained at 12 K (Fig. 2) is in reasonable accord with the first option: the local symmetry (Fig. 1) is quite close to being cubic in this monoclinic SmP_5O_{14} crystal and it is not possible to separate the lines further for the first three bands, although in principle this might have been possible because the symmetry is not strictly cubic. The shape of the co-ordination polyhedron of the eight oxygen atoms surrounding a Sm^{3+} ion, shown in Fig. 1c, can be thought of as a distorted cube. The symmetry of the real co-ordination polyhedra is clearly lower than that of the ideal antiprism, which has D_{4d} symmetry. Thus an interpretation of the fluorescence spectral lines for the SmP_5O_{14} crystal is that the local symmetry around the Sm^{3+} ion is close enough to being cubic to prevent separation into the extra lines, which would be anticipated for the actual lower symmetry structure.

At 12 K there is a systematic disappearance of the shortest wavelength lines of each fluorescence band, which is attributable to a decreasing population of higher crystal field levels, which can be occupied at ambient temperature. However, this is not the only possible explanation of the line disappearance at low temperatures. Another might have been transitions from the $^4F_{3/2}$ level, which is located at 18 860 cm^{-1} in the free ion (that is higher than the $^4G_{5/2}$ level) down to the multiplets that comprise the ^6H_J. However, calculations, which need not be detailed here, made of the fluorescence spectral line positions, which would occur in this case, show that they are on the *higher*, rather than the *lower* wavelength side, of each of the five bands. Furthermore, the $^4F_{3/2}$ level is a singlet in an environment of cubic symmetry; so a transition from it to the $^6H_{5/2}$ (which is a doublet in cubic symmetry) would give only

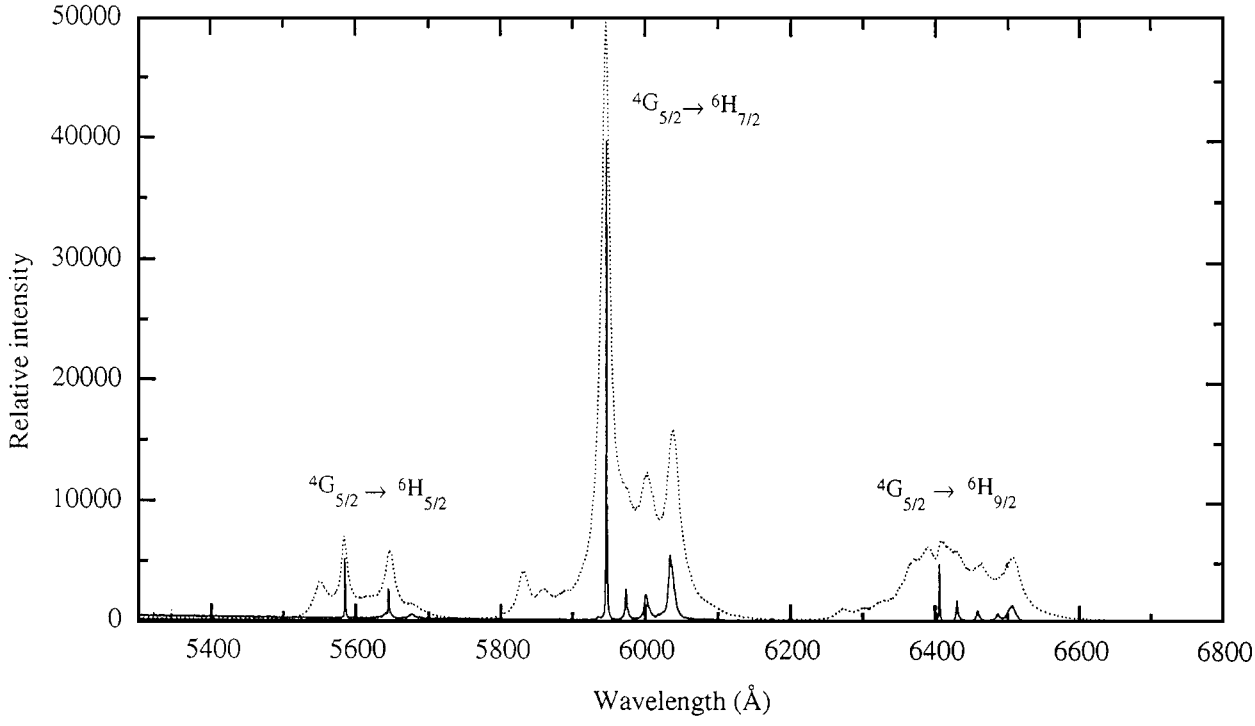

(a)

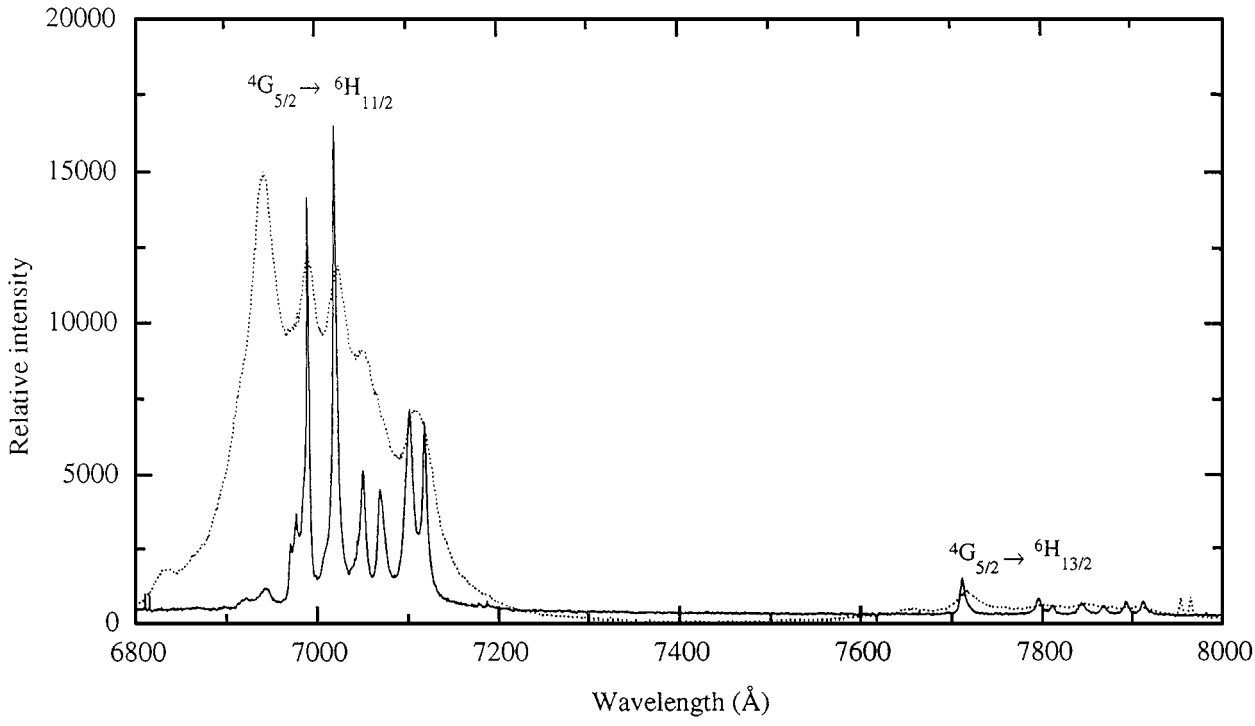

(b)

Figure 2 The fluorescence spectrum of monocrystalline SmP_5O_{14} at 12 K (—) and 300 K (···) excited using the blue 476.5 nm (4765 Å) argon ion laser line. The laser power used to obtain the shorter wavelength region of the spectrum shown in (a) was much less than that used to excite the longer wavelength region in (b).

two lines in the vicinity of 530 nm (5302 Å). This has been tested experimentally. Due to the low level of the signal, to obtain the fluorescence in this region, it proved necessary to use wider slit widths (both 200 μm) and higher laser power (200 mW) instead of the values of 100 μm and 100 mW employed to determine the spectrum shown in Fig. 2. Fig. 3 shows this particular part of the fluorescence spectrum at 300 K; it consists of at least four observable lines (listed in Table I), which have much lower intensities than those shown in Fig. 2; these lines do not exist at 12 K. Transitions from the $^4F_{3/2}$ level cannot correspond to the fluorescence lines that disappear at low temperature because (i) those vanishing lines are much stronger at room temperature than can be expected of transitions from $^4F_{3/2}$ and (ii) their location on the longer wavelength side of each band is not consistent with the observation that the disappearing lines are on the shorter wavelength side.

TABLE I Fluorescence peak wavelengths (λ) of the SmP_5O_{14} crystal at 12 K, 300 K and under a 50 kbar pressure at 292 K in a diamond anvil cell

	Fluorescence line wavelengths of SmP_5O_{14}, λ			
Transition assignments	At 12 K[a] nm (Å)	At 300 K, atmospheric P nm (Å)[a]	At 292 K, 50 kbar nm (Å)[a]	Pressure derivative at 92 K, $d\lambda/dP$ nm $kbar^{-1}$ (Å $kbar^{-1}$)[a]
$^4F_{3/2} \rightarrow {}^6H_{5/2}$	Absent	525.65 (5256.5)		
		526.03 (5260.3)		
		531.43 (5314.3)		
		534.27 (5342.7)		
$^4G_{5/2} \rightarrow {}^6H_{5/2}$	—	555.06 (5550.6)	—	
	558.47 (5584.7)	558.41 (5584.1)	560.15 (5601.5)	0.0316 (0.316)
	564.14 (5641.4 (s))	—	—	
	564.52 (5645.2)	564.65 (5646.5)	565.64 (5656.4)	0.015 (0.155)
	567.60 (5676.0 (weak))	567.47 (5674.7)	—	
$^4G_{5/2} \rightarrow {}^6H_{7/2}$	—	583.15 (5831.5)	585.45 (5854.5)	0.0401 (0.401)
	—	585.89 (5858.9)	—	
	—	588.85 (5888.5)	—	
	593.40 (5934.0 (s))	—	—	
	594.74 (5947.4 (strongest))	594.60 (5946.0)	596.44 (5964.4)	0.0307 (0.307)
	597.37 (5973.7)	597.15 (5971.5)	598.44 (5984.4)	
	600.09 (6000.9)	600.38 (6003.8)	602.10 (6021.0)	0.0271 (0.271)
	602.62 (6026.2 (s))	—	—	
	603.50 (6035.0)	603.80 (6038.0)	605.59 (6055.9)	0.0284 (0.284)
$^4G_{5/2} \rightarrow {}^6H_{9/2}$	—	627.11 (6271.1)	630.56 (6305.6)	
	—	638.81 (6388.1)	640.72 (6407.2)	
	640.61 (6406.1)	640.86 (6408.6)	644.38 (6443.8)	
	643.00 (6430.0)	—	—	
	645.91 (6459.1)	646.41 (6464.1)	647.71 (6477.1)	
	648.67 (6486.7)	—	—	
	650.61 (6506.1)	650.70 (6507.0)	652.20 (6522.0)	
$^4G_{5/2} \rightarrow {}^6H_{11/2}$	—	682.96 (6829.6)	Too weak to follow under pressure	
	—	686.62 (6866.2)		
	692.10 (6921.0)	686.62 (6866.2)		
	694.30 (6943.0)	694.25 (6942.5)		
	697.00 (6970.0)	—		
	697.73 (6977.3)	—		
	699.10 (6991.0)	699.20 (6992.0)		
	702.15 (7021.49)	702.54 (7025.4)		
	705.11 (7051.1)	705.11 (7051.1)		
	707.01 (7070.1)	—		
	710.22 (7102.2)	710.73 (7107.3)		
	711.84 (7118.4)	—		
$^4G_{5/2} \rightarrow {}^6H_{13/2}$	—	765.81 (7658.1)	Too weak to follow under pressure	
	771.13 (7711.3)	771.72 (7717.2)		
	779.54 (7795.4)	779.91 (7799.1)		
	781.12 (7811.2)	—		
	784.31 (7843.1)	784.68 (7846.8)		
	786.78 (7867.8)	—		
	789.26 (7892.6)	—		
	791.13 (7911.3)	—		

[a]Values in parentheses are in Angstroms.

In principle, anti-Stokes' Raman spectra induced from the fluorescent lines could be the source of the peaks seen on the shorter wavelength side of the bands at room temperature: anti-Stokes' lines would disappear at low temperature. For example, if the strongest fluorescence line at 594.74 nm (5947.4 Å) were to be an excitation source of an intrinsic Raman spectrum, it would then be responsible for the peaks on the short wavelength side of the first two bands. To test this possibility, Raman spectrum measurements have been made as a function of temperature; this has become a study in itself and fuller details will be published elsewhere. The experimental Raman spectra of SmP_5O_{14}, shown at 300 and 12 K in Fig. 4, show a large number of sharp lines as would be expected: the monoclinic crystal structure is consistent with 240 normal modes at the Brillouin zone centre, although since the structure is centrosymmetric, the infrared active modes are Raman inactive. Comparison between the spectra measured at 12 and 300 K, shows some marked changes; the two spectral lines located above the frequency shift 1400 cm^{-1} in the spectrum of the 300 K temperature are absent at 12 K. These two lines are related to the fluorescence of the Sm^{3+} ion; they did not retain the same frequency shift locations when the spectrum was excited using the 476.5 nm (4765 Å) laser line. At 300 K the Raman lines of the crystal located at 362, 674 and 718 cm^{-1} have half-widths of about 10, 14 and 7 cm^{-1}, respectively, yet at 12 K these lines have half-widths around 3, 6 and 5 cm^{-1}, respectively. The highest half-width (14 cm^{-1}) is about 0.4 nm (4 Å) for the Raman lines. However, the fluorescence lines, which are assumed to be related

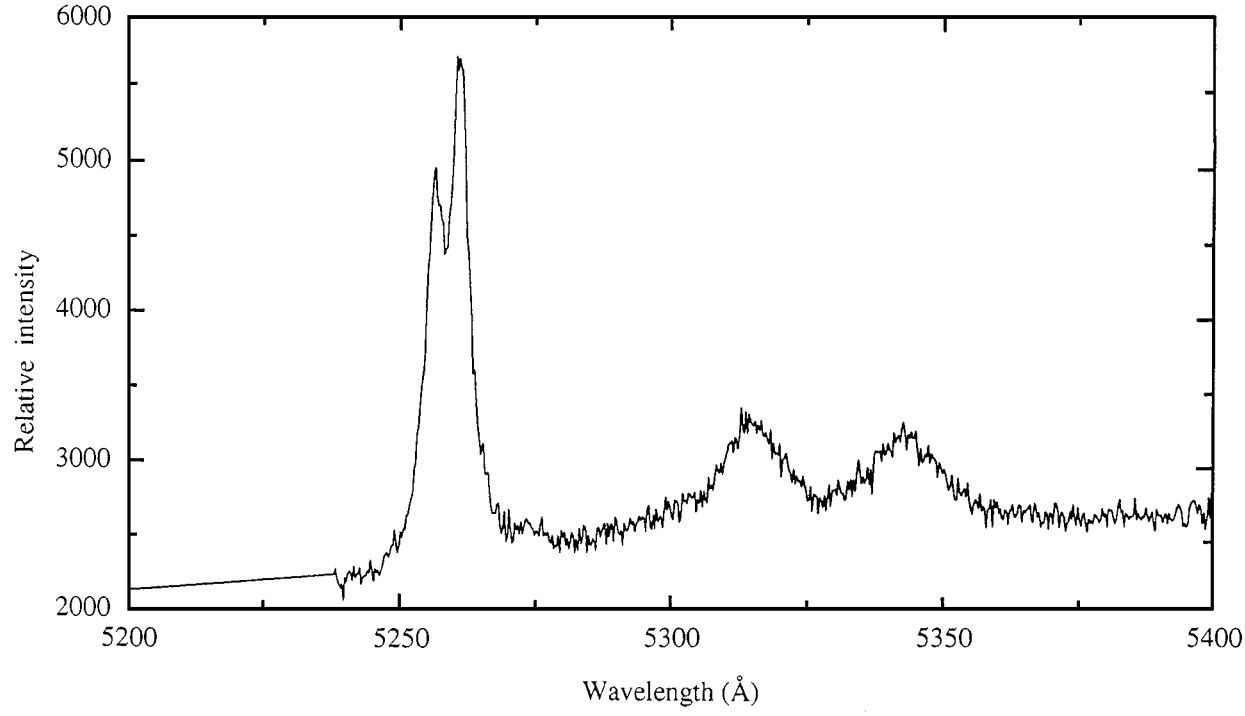

Figure 3 Low wavelength region fluorescence of monocrystalline SmP_5O_{14} at 300 K (determined using a wider 200 μm slit width in the monochromator).

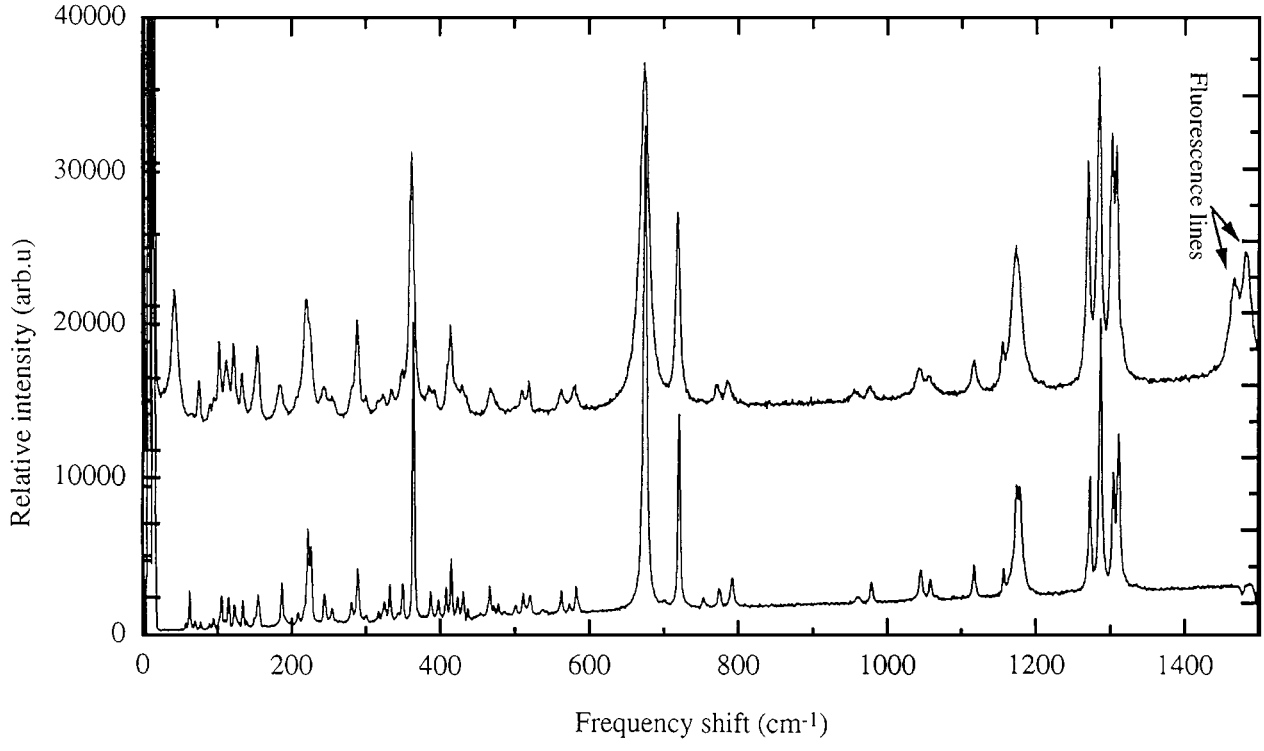

Figure 4 The Raman spectrum of samarium pentaphosphate crystal (SmP_5O_{14}) measured at 300 K (upper spectrum) and 12 K (lower spectrum).

to intrinsic Raman spectrum of the crystal, are about 2 nm (20 Å) wide at 300 K (Fig. 2a): much wider than the half-width of the Raman lines. Hence, although the lines that disappear at low temperature do fit some positions, which would be expected for anti-Stokes' lines of the crystal, at room temperature they are much too strong and wide for them to be Raman lines induced by an intrinsic fluorescent source.

The effect of temperature on the low frequency Raman mode located at 42 cm^{-1} is evident in Fig. 4; it has shifted to 62 cm^{-1} at 12 K; this renormalization demonstrates instability of the corresponding optical phonon mode in SmP_5O_{14}. Similar mode softening, observed in LaP_5O_{14}, NdP_5O_{14}, PrP_5O_{14} and TbP_5O_{14}, has been associated with second order, ferroelastic transitions in these crystals with a symmetry change

$mmm \rightarrow 2/m$ (or $D_{2h}^7 \rightarrow C_{2h}^5$ [20–24]. The softer optic mode in the RP_5O_{14} crystals has the same B_{2g} symmetry as the spontaneous e_5 monoclinic shear and so, as the ferroelastic transition temperature, T_c, is approached from above, this optic mode softens and the coupled elastic stiffness tensor component (c_{55}) is expected to go towards zero. Thus the ferroelastic transition is driven by softening of this acoustic phonon mode. The observation of the change in the character of the fluorescence (Fig. 2) with temperature, which is consistent with an alteration in the local symmetry of the rare earth ions – requiring a slight structural rearrangement of the linked PO_4 tetrahedra – may be associated with the phonon mode softening in the SmP_5O_{14} crystal.

3.1.2. Fluorescence spectrum of samarium metaphosphate glasses

Phosphate glasses can be constructed from several types of building units: (i) a branching PO_4 unit in which three oxygen atoms are shared with neighbouring PO_4 units, (ii) a middle unit in which two oxygen atoms are shared with neighbouring PO_4, and there is one negative charge which is neutralized by a cation, (iii) an end unit with one oxygen shared with another PO_4 and having two negative charges. The skeleton is made from pairs of PO_4 tetrahedra sharing only one corner. EXAFS structural studies carried out recently on a range of rare earth metaphosphate $R(PO_3)_3$ glasses modified using the rare earth oxides Nd_2O_3, Eu_2O_3, Gd_2O_3, Tb_2O_3, Ho_2O_3 and Pr_6O_{11} have established that the glass skeleton is made up from linked PO_4 tetrahedra [25, 26]. The trivalent rare earth ions occupy sites with an average co-ordination number $6 < N < 8$ inside a skeleton of linked PO_4 tetrahedra, with an average R–O distance of approximately 0.23 nm (2.30 Å) following the lanthanide contraction, and an R–P distance of approximately 0.29 nm (2.90 Å). An EXAFS study has shown that the $(Sm_2O_3)_{0.248}(P_2O_5)_{0.752}$ glass has a similar structure [27]. One of the four oxygen atoms in a PO_4 tetrahedron is doubly bonded to the phosphorus and may not take part in the network bonding. The rare earth ions occupy sites with an average co-ordination number of surrounding oxygen atoms in the range $6 \leq N \leq 8$. This is a common range for oxygen co-ordination in rare earth oxides and is consistent with a cubic or "pseudocubic" local environment for the R^{3+} ions. There is no evidence from EXAFS for rare earth ions being adjacent to each other in the metaphosphate glasses. Further structural indications can be obtained from the fractal bond connectivity $4C_{44}/B$ [28, 29]. Ultrasonic pulse echo measurements have shown that the elastic stiffnesses of the glass of composition $(Sm_2O_3)_{0.248}(P_2O_5)_{0.752}$ studied here are C_{44} and the bulk modulus, B, and these are equal to 68.7 and 39.1 GPa, respectively, giving a fractal bond connectivity of 2.3, indicating that the connectivity of this glass falls between a two- and three-dimensional character. In the Reisfeld model [6], a rare earth ion in a phosphate glass is considered to occupy the centre of a distorted cube comprised of four phosphate tetrahedrons. An edge of the cube is formed by two oxygen atoms belonging to a single tetrahedron. The co-ordination number of the rare earth ion in such an arrangement is eight oxygen atoms. This model is consistent with the EXAFS structural studies.

By comparing the fluorescence for the samarium metaphosphate glass with that of the pentaphosphate crystal useful insight can be gained about how the local symmetries of Sm^{3+} ions affect the fluorescence in the glass. The fluorescence of the samarium metaphosphate glass at room temperature (dotted line) is overlapped on the fluorescence spectrum at 10 K (solid line) in Fig. 5. As it does for the SmP_5O_{14} crystal (Fig. 2 and Table I), the fluorescence of the glass falls naturally into five bands, although, due to the existence of non-uniform, non-identical ligand fields caused by slightly different values of rare-earth oxygen distances, they are now much broadened and the individual lines are not resolved. Thus the fluorescence of the glass originates in the same Sm^{3+} transitions as in the crystal, namely those listed in Table I. For the glass at both room temperature and 10 K the intensity of the $^4G_{5/2} \rightarrow {}^6H_{9/2}$ band is not much higher than that of the $^4G_{5/2} \rightarrow {}^6H_{7/2}$ band (Fig. 5a). For the crystal, by contrast the intensities of these two fluorescence bands are very different (Fig. 2a), due to the operation of selection rules. Comparison between the spectra of the glass and the crystal both at room temperature and 12 K show that the whole spectrum of the glass is shifted towards longer wavelength. A comparison between fluorescence lines in the first three bands for the crystal and the glass at 12 K shows the shifts clearly (Fig. 6). In the first band the shift is about 3.3 nm (33 Å), in the second is about 2.4 nm (24 Å), and in the third band is about 3.3 nm (33 Å). The shift occurs even in the longer wavelength band region, but there its measurement is not reliable due to the low-level signal, the breadth of the bands and also because the higher energy levels are more susceptible to crystal field effects. This shift towards the longer wavelength for the glass is an indication of a stronger ligand field around the Sm^{3+} ion in the glass than in the crystal. This is as expected because the metaphosphate has a higher Sm^{3+} ion concentration than that of the pentaphosphate crystal.

When the glass is cooled down to 10 K, one obvious feature is the disappearance of the tail on the short wavelength side for each of the five fluorescence bands (solid line in Fig. 5). This appears to be a counterpart of the disappearance of the shorter wavelength lines in the crystal fluorescence as the temperature is reduced (Fig. 2); which, as for the crystalline SmP_5O_{14}, can be attributed to a decreasing population of higher energy crystal field levels that can be occupied at ambient temperature.

3.2. The effect of hydrostatic pressure on fluorescence of SmP_5O_{14} crystal and $(Sm_2O_3)_{0.248}(P_2O_5)_{0.752}$ glass

In fact vitreous samarium metaphosphate shows anomalous elastic behaviour as a function of temperature and pressure [17, 30, 31]. The hydrostatic pressure derivatives $(\partial C_{11}/\partial P)_{T,P=0}$ and $(\partial C_{44}/\partial P)_{T,P=0}$ of

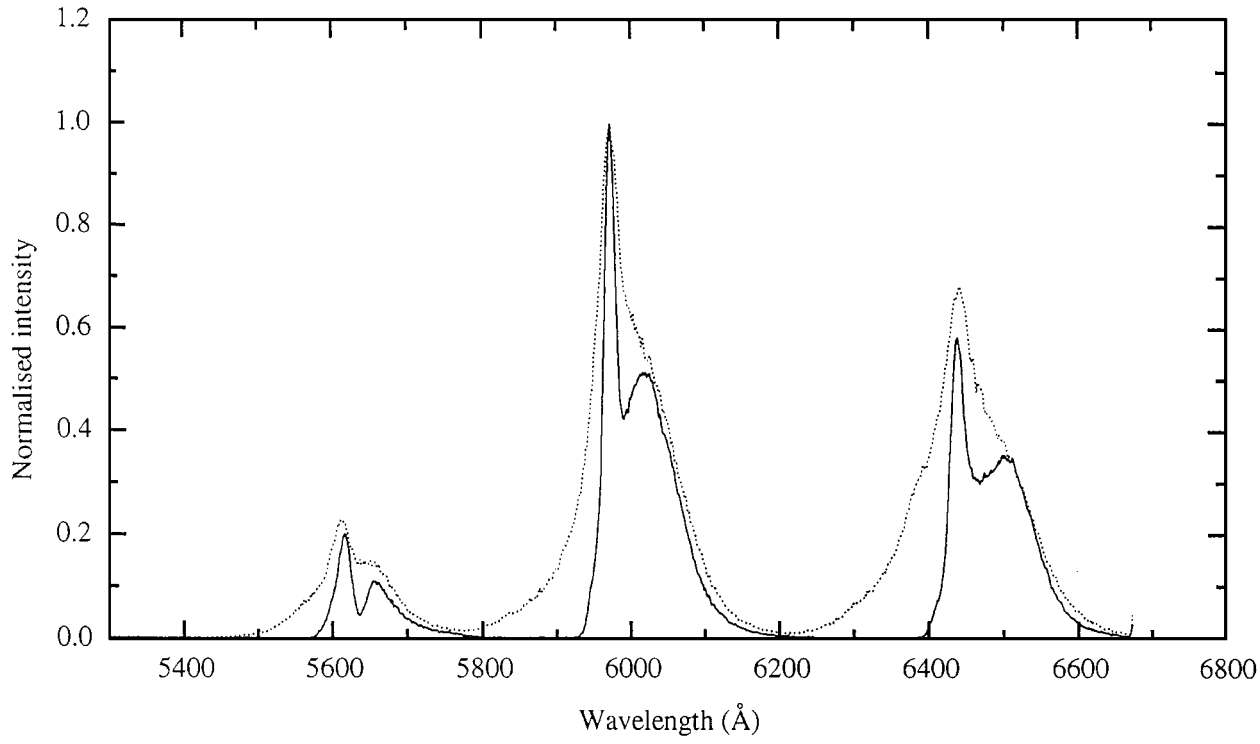

(a)

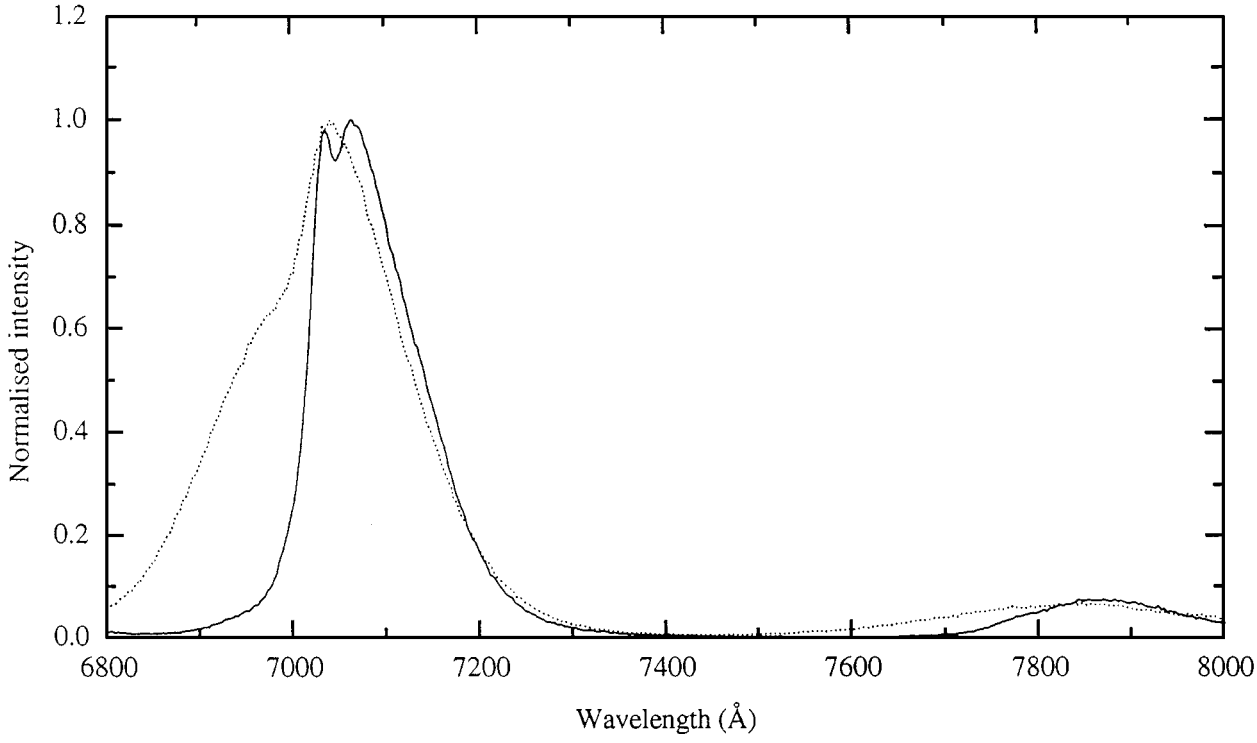

(b)

Figure 5 The fluorescence spectrum of $(Sm_2O_3)_{0.248}(P_2O_5)_{0.752}$ glass at 10 K (—) and 300 K (···) excited using the blue 476.5 nm (4765 Å) argon ion laser line. The laser power used to obtain the shorter wavelength region of the spectrum shown in (a) was much less than that used to excite the longer wavelength portion in (b).

the elastic stiffness tensor components are negative: the long-wavelength acoustic modes soften under pressure. The hydrostatic pressure derivative $(\partial B^S/\partial P)_{T,P=0}$ of the adiabatic bulk modulus, B^S, is negative; the glass becomes easier to squeeze when subjected to high pressure [17]. The physical origin of this acoustic mode softening was suggested to be non-linear acoustic contributions from bending vibrations of the bridging oxygen atoms, which correspond to transverse motion against small force constants, or rotations of the coupled PO_4 tetrahedra. Since application of pressure can induce acoustic mode softening, its effects on the laser induced fluorescence have been examined to find out if there is any influence on the optical modes.

The effect of pressure on the wavelengths of the laser induced fluorescence lines of the SmP_5O_{14} crystal can

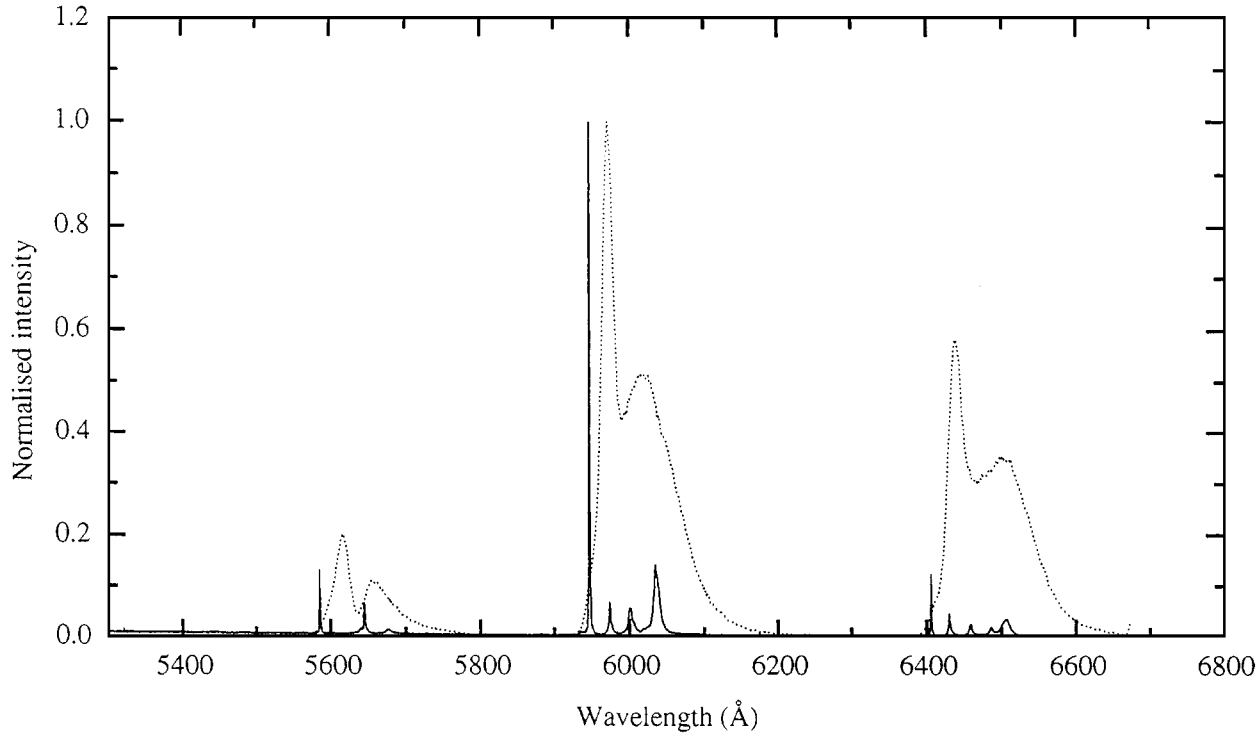

Figure 6 Comparison between the fluorescence spectra at 12 K of the SmP_5O_{14} crystal (—) and $(Sm_2O_3)_{0.248}(P_2O_5)_{0.752}$ glass (· · ·) in the first three bands.

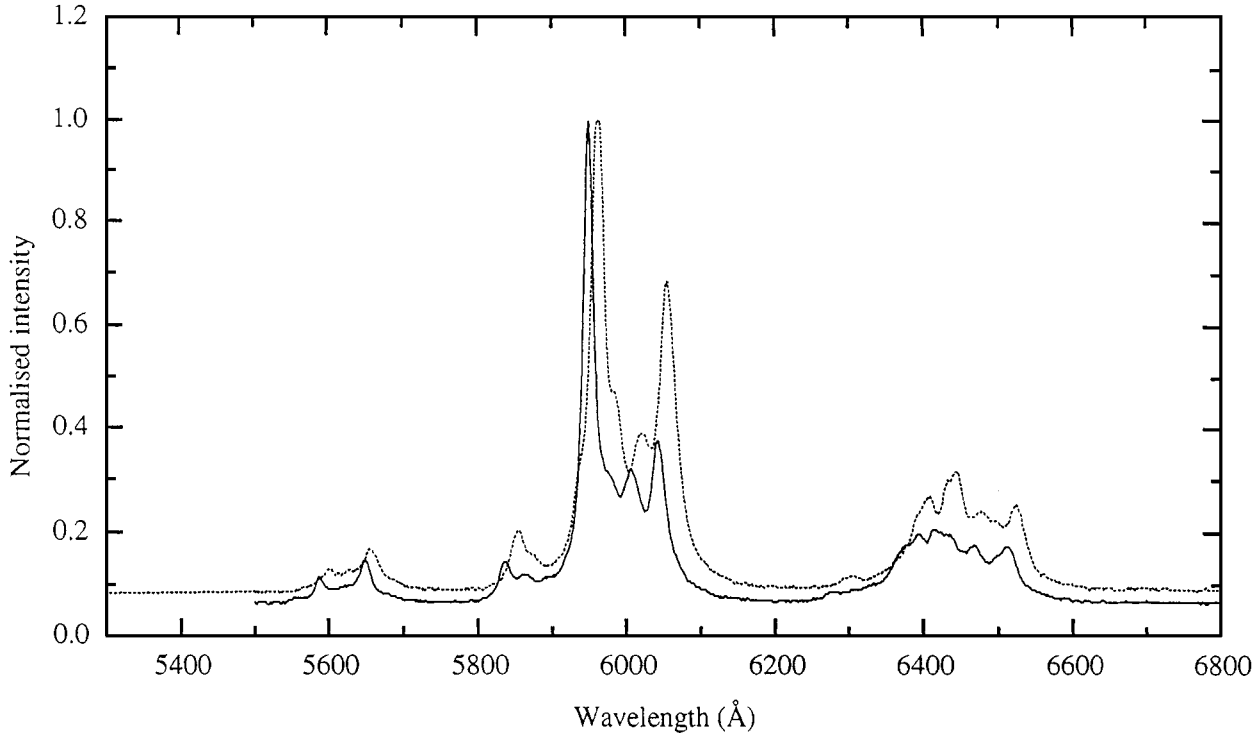

Figure 7 The effect of pressure, 1 bar (—) and 50 kbar (· · ·) on the fluorescence spectrum in the short wavelength region for monocrystalline SmP_5O_{14} at 292 K.

be seen in Fig. 7, which shows the fluorescence spectrum obtained under a pressure of 50 kbar superimposed on that determined at atmospheric pressure. The positions of the fluorescence lines of the crystal under pressure of 50 kbar and room temperature are given in Table I. The wavelength, λ, of the lines increases approximately linearly with pressure; as an example, the effect of pressure on the lines in the $^4G_{5/2} \rightarrow {}^6H_{7/2}$ transition band is shown in Fig. 8. Under pressure all lines shift towards longer wavelengths; the pressure derivatives ($d\lambda/dP$) determined from the experimental data are listed in Table I. Bands sited at wavelengths of more than 680 nm (6800 Å) have low intensity and overlap with ruby chip fluorescence lines and it was not possible to measure their pressure shifts in the DAC. An experimental feature shown by SmP_5O_{14} is polarization

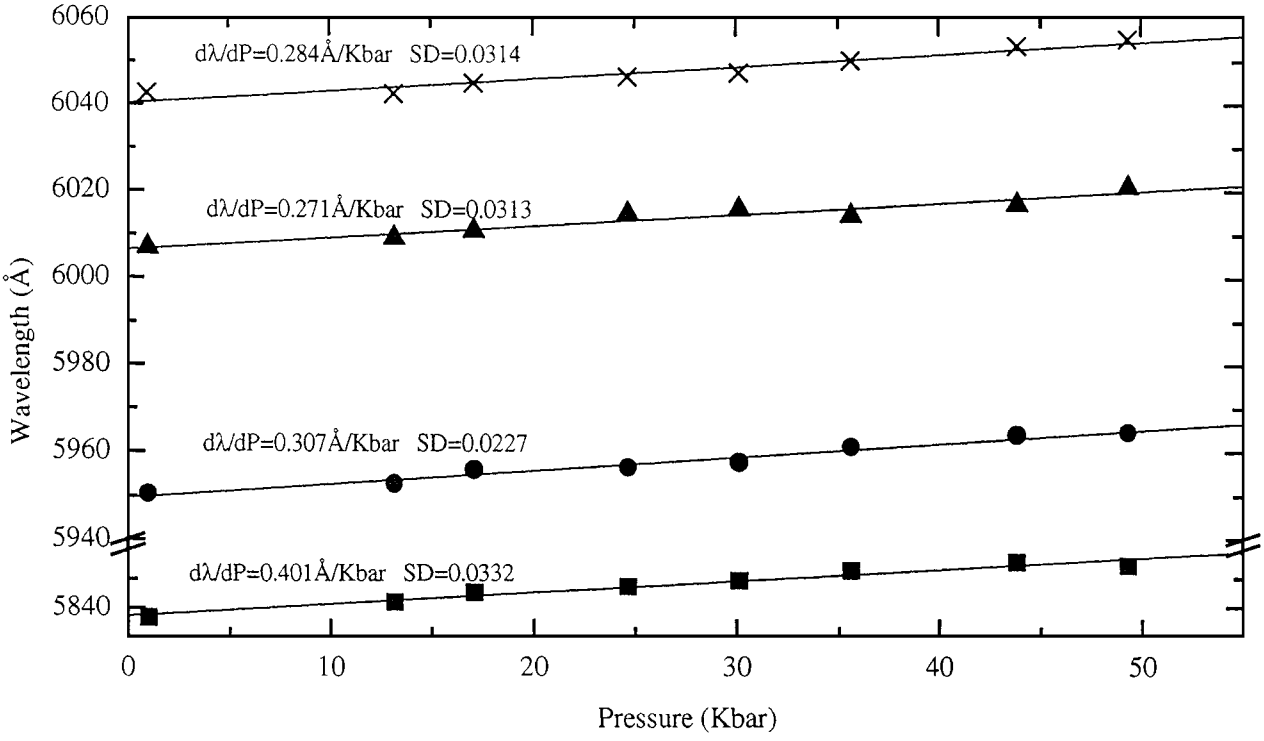

Figure 8 The effect of pressure on the wavelength of the lines in the $^4G_{5/2} \rightarrow {}^6H_{7/2}$ transition band (see Table I, column 3) of SmP_5O_{14} crystal at 292 K. The wavelengths of the lines at 300 K are: (□) 583.15 nm (5831.5 Å); (○) 594.6 nm (5946.0 Å); (△) 600.38 nm (6003.8 Å); (+) 603.8 nm (6038.0 Å).

of some of the fluorescence lines in the bands, when the crystal is oriented at different angles. An increase in the relative intensities of some of the lines (555, 603.8 and 640.8 nm; 5550, 6038 and 6408 Å) at 50 kbar is due to a change of the orientation of the sample during application of pressure; these lines are directionally polarized. The most pronounced polarization effects observed were a moderate increase in intensity of the lines at 555 nm (5550 Å; first band), 603.8 nm (6038 Å; second band), 640.8 nm (6408 Å; third band), while the remainder keep their original intensities in all other orientations. The effect of pressure on the lines associated

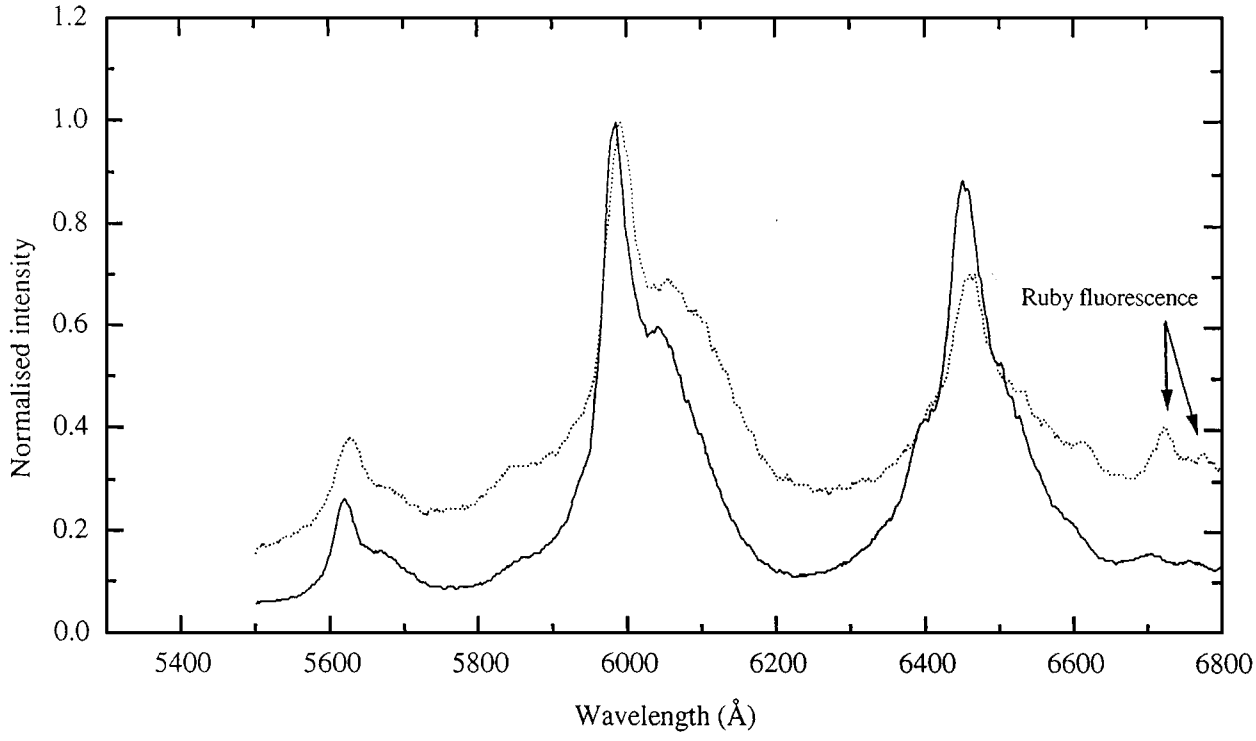

Figure 9 The effect of pressure, 1 bar (—) and 50 kbar (· · ·), on the fluorescence spectrum of $(Sm_2O_3)_{0.248}(P_2O_5)_{0.752}$ glass (only the short wavelength region) at 292 K.

with fluorescence is a stiffening. This is in contrast to the softening with reducing temperature observed for certain optic modes in the Raman spectra.

The fluorescence spectrum of the samarium metaphosphate glass under atmospheric pressure and room temperature (solid line) is overlapped onto that obtained at 50 kbar in the DAC (dotted line) in Fig. 9. The small peaks in the vicinity of 670 nm (6700 Å) are ruby fluorescence lines. Under pressure there are small changes in the shape, the width or the positions of the broad fluorescence peaks but the glass withstands high pressure without marked change in its fluorescence properties. Neither the crystal nor the glass show any mode softening effects under pressure.

4. Conclusions

1. The laser induced fluorescence spectra of metaphosphate glass of composition $(Sm_2O_3)_{0.248}(P_2O_5)_{0.752}$ and an pentaphosphate crystal (SmP_5O_{14}) at room temperature show that in both materials the samarium ions are in the 3+ state.

2. The fluorescence spectrum of samarium in the SmP_5O_{14} crystal splits into five groups of well separated bands. The number of lines in each band indicates that the local symmetry is close enough to being cubic to preclude line separation. This is consistent with the crystal structure; the Sm^{3+} ions can be likened to a rough approximation to be at the centre of a pseudocube comprised of eight oxygen atoms belonging to PO_4 tetrahedra.

3. When the temperature of the crystal is reduced to 12 K, some of the fluorescence lines at the short wavelengths in each band disappear due to decreasing population of higher energy levels.

4. The fluorescence spectrum of samarium ion in the $(Sm_2O_3)_{0.248}(P_2O_5)_{0.752}$ glass also splits into five groups of well separated bands. When the glass is cooled down to 10 K, there is disappearance of the tail on the short wavelength side for each of the five fluorescence bands. This is a counterpart of the disappearance of the shorter wavelength lines in the crystal fluorescence at low temperature.

5. When a high pressure is applied to the crystal, the fluorescence lines in the first two bands shift towards longer wavelengths with pressure derivatives $(d\lambda/dP)$ ranging between 0.015 and 0.04 nm kbar^{-1} (0.15 and 0.4 Å kbar^{-1}).

6. The effects of pressure on the laser-induced fluorescence of the SmP_5O_{14} crystal and the $(Sm_2O_3)_{0.248}(P_2O_5)_{0.752}$ glass have been measured; neither material shows any mode softening or other effects under pressure that might be associated with any phase transition.

7. Softening with decreasing temperature of a low frequency Raman mode has been observed, which indicates that, like other RP_5O_{14} crystals, SmP_5O_{14} undergoes a ferroelastic phase transition.

Acknowledgements

We are grateful to the Johnson Matthey Technology Centre (A. Pratt) for support of our programme of work and to Dr H. B. Senin (Universiti Pertanian Malaysia) for analysing the glass samples. We are also grateful to the EPSRC (in the form of a ROPA award) and NATO (Scientific and Environmental Affairs Division, Grant number CRG960584) for financial support.

References

1. P. J. FORD, C. D. GRAHAM, G. A. SAUNDERS, H. B. SENIN and J. R. COOPER, *J. Mater. Sci. Lett.* **13** (1994) 697.
2. G. A. SAUNDERS, G. D'ANGELO, G. TRIPODO and G. CARINI, in Proceedings of the Conference on Non-equilibrium Phenomena in Supercooled Fluids, Glasses and Amorphous Materials, Pisa (1995) in press.
3. G. CARINI, G. D'ANGELO, G. TRIPODO, A. BARTOLETTA, A. FONTANA, F. ROSSI and G. A. SAUNDERS, *Euro Phys. Lett.* **40** (1997) 435.
4. W. A. PHILLIPS (Ed.) "Amorphous Solids: Low Temperature Properties" (Springer, Berlin, 1981).
5. U. BUCHENAU, *Europhys. News* **24** (1993) 77.
6. R. REISFELD and Y. ECKSTEIN, *J. Solid State Chem.* **5** (1972) 174.
7. R. REISFELD, R. A. VELAPOLDI, L. BOEHM and M. ISH-SHALOM, *J. Phys. Chem.* **75** (1971) 3981.
8. M. BEUCHER, "Les Elements des Terres Rares," Coll. No. 180, Vol. 1, (1970) pp. 331.
9. H. G. DANIELMEYER and H. P. WEBER, *IEEE J. Quantum Electron.* **QE8** (1972) 805.
10. H. P. WEBER, T. C. DAMEN, H. G. DANIELMEYER and B. C. TOFIELD, *Appl. Phys. Lett.* **22** (1972) 534.
11. W. A. RUNCIMAN, *Reports Prog. Phys.* **21** (1958) 30.
12. K. HIRAO and N. SOGA, *J. Amer. Ceram. Soc.* **68** (1985) 515.
13. T. F. BELLIVEAU and D. J. SIMKIN, *J. Non-Cryst. Solids.* **110** (1989) 127.
14. H. M. FAROK, G. A. SAUNDERS, W. POON and H. VASS, *ibid.* **142** (1992) 175.
15. H. BETHE, *Annals. Phys.* **3** (1929) 133.
16. W. A. RUNCIMAN, *Phils. Mag.* **1** (1956) 1075.
17. A. MIERZEJEWSKI, G. A. SAUNDERS, H. A. A. SIDEK and B. BRIDGE, *J. Non-Cryst. Solids* **104** (1988) 323.
18. G. J. PIERMARINI, S. BLOCK and J. D. BARNETT, *J. Appl. Phys.* **44** (1973) 5377.
19. G. J. PIERMARINI and S. BLOCK, *Rev. Sci. Instrum.* **46** (1975) 973.
20. G. ERRANDONES and J. SAPRIEL, *Solid State Commun.* **32** (1979) 391.
21. H. SCHULZ, K. H. THIEMANN and J. FENNER, *Mater. Res. Bull.* **9** (1974) 1525.
22. J. P. BUDIN, A. MILATOS ROUFOS, N. DUC CHINH and G. LE ROUX, *J. Appl. Phys.* **46** (1975) 2867.
23. H. P. WEBER, B. C. TOFIELD and P. F. LIAO, *Phys. Rev. B* **11** (1975) 1152.
24. T. KOBAYASHI, T. SAWADA, H. IKEO, K. MUTO and J. KAI, *J. Phys. Soc. Jpn* **40** (1976) 595.
25. D. BOWRON, R. J. NEWPORT, B. D. RAINFORD, G. A. SAUNDERS and H. B. SENIN, *Phys. Rev. B* **51** (1995) 5739.
26. D. T. BOWRON, R. J. NEWPORT, G. A. SAUNDERS, H. B. SENIN and B. D. RAINFORD, *ibid.* **53** (1996) 5268.
27. R. ANDERSON, T. BRENNAN, G. MOUNTJOY, R. J. NEWPORT and G. A. SAUNDERS, to be published.
28. D. J. BERGMAN and Y. KANTOR, *Phys. Rev. Lett.* **53** (1984) 511.
29. R. BOGUE and R. J. SLADEK, *Phys. Rev. B* **42** (1990) 5280.
30. G. CARINI, M. CUTRONI, G. D'ANGELO, M. FEDERICO, G. GALLI, G. TRIPODO, G. A. SAUNDERS and Q. WANG, *J. Non-Cryst. Solids* **121** (1990) 288.
31. H. B. SENIN, Q. WANG, G. A. SAUNDERS and E. F. LAMBSON, *ibid.* **152** (1993) 83.

Received 13 January
and accepted 3 September 1998